Journal of Medicinal Chemistry

Article

Cite This: J. Med. Chem. 2017, 60, 10257−10267

pubs.acs.org/jmc

Novel Aryl Substituted Pyrazoles as Small Molecule Inhibitors of Cytochrome P450 CYP121A1: Synthesis and Antimycobacterial Evaluation

Ismail M. Taban,[†] Hosam E. A. E. Elshihawy,[‡] Beyza Torun,[†,§] Benedetta Zucchini,[†,∥] Clare J. Williamson,[†] Dania Altuwairigi,[†] Adeline S. T. Ngu,[†] Kirsty J. McLean,[⊥] Colin W. Levy,[⊥] Sakshi Sood,[#] Leonardo B. Marino,[○] Andrew W. Munro,[⊥] Luiz Pedro S. de Carvalho,[#] and Claire Simons*[,†]

[†]School of Pharmacy & Pharmaceutical Sciences, Cardiff University, King Edward VII Avenue, Cardiff CF10 3NB, U.K.

[‡]Department of Organic Chemistry, Faculty of Pharmacy, Suez Canal University, Ismalia, Egypt

[§]Faculty of Pharmacy, Department of Pharmaceutical Chemistry, Ankara University, 06100 Tandogan, Ankara, Turkey

[∥]Department of Pharmaceutical Sciences, University of Perugia, Via del Liceo, 1-06123 Perugia, Italy

[⊥]Manchester Institute of Biotechnology, School of Chemistry, The University of Manchester, 131 Princess Street, Manchester M1 7DN, U.K.

[#]Mycobacterial Metabolism and Antibiotic Research Laboratory, The Francis Crick Institute, 1 Midland Road, London NW1 1AT, U.K.

[○]Faculty of Pharmaceutical Sciences, UNESP-Univ Estadual Paulista, Araraquara, São Paulo14801-902, Brazil

Supporting Information

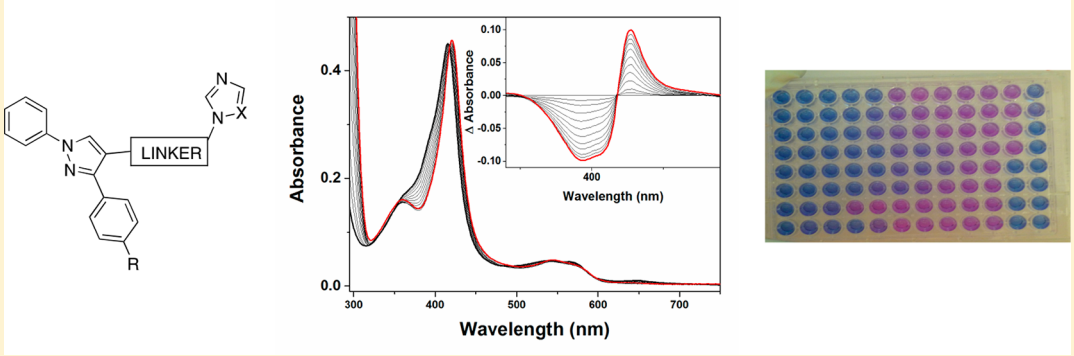

ABSTRACT: Three series of biarylpyrazole imidazole and triazoles are described, which vary in the linker between the biaryl pyrazole and imidazole/triazole group. The imidazole and triazole series with the short $-CH_2-$ linker displayed promising antimycobacterial activity, with the imidazole$-CH_2-$ series (**7**) showing low MIC values (6.25−25 μg/mL), which was also influenced by lipophilicity. Extending the linker to $-C(O)NH(CH_2)_2-$ resulted in a loss of antimycobacterial activity. The binding affinity of the compounds with CYP121A1 was determined by UV−visible optical titrations with K_D values of 2.63, 35.6, and 290 μM, respectively, for the tightest binding compounds **7e**, **8b**, and **13d** from their respective series. Both binding affinity assays and docking studies of the CYP121A1 inhibitors suggest type II indirect binding through interstitial water molecules, with key binding residues Thr77, Val78, Val82, Val83, Met86, Ser237, Gln385, and Arg386, comparable with the binding interactions observed with fluconazole and the natural substrate dicyclotyrosine.

INTRODUCTION

Tuberculosis (TB) is endemic in numerous countries of the developing world, and serious issues are caused by infection with drug- (and multidrug-) resistant strains of the causative bacterium *Mycobacterium tuberculosis* (Mtb) and by the common occurrence of HIV coinfection as a result of the high susceptibility of immunocompromised individuals to TB infection.[1,2] The global impact of TB is evident from the World Health Organization data, which reported that, in 2015, 1.8 million people died from TB and approximately 2 billion people, a third of the world's population, were infected with latent TB.[2] This disease has a global impact, and the "deadly synergy" of coinfection with TB and HIV has serious life-

Received: October 20, 2017
Published: November 29, 2017

DOI: 10.1021/acs.jmedchem.7b01562
J. Med. Chem. 2017, 60, 10257−10267

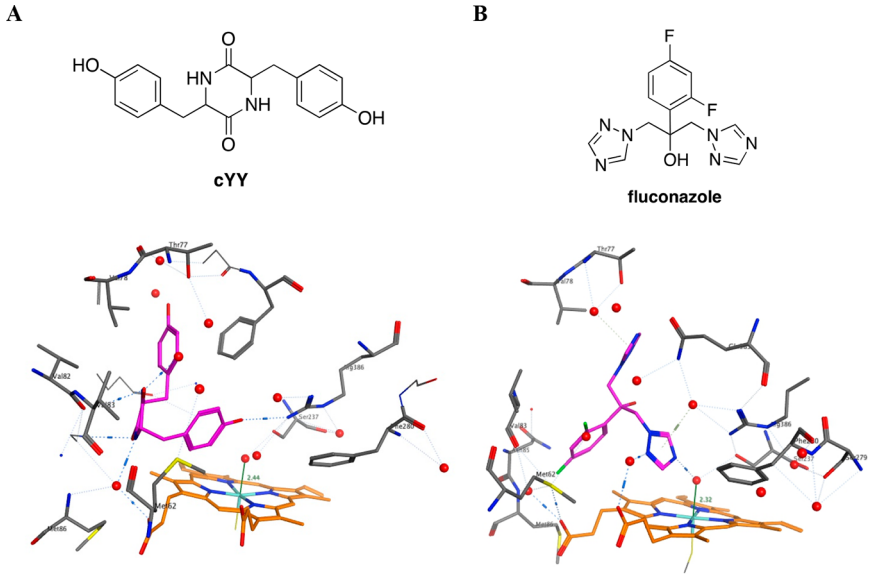

Figure 1. Crystal structures of CYP121A1 cocrystallized with (A) cYY (PDB 3GH) and (B) fluconazole (PDB 2IJ7). The natural substrate and fluconazole both interact indirectly with the heme via interstitial water molecules with key amino acids identified.

limiting consequences for individuals who do not receive the relevant therapeutics in a timely manner.[1,2]

Challenges associated with the current antibiotic therapy include drug intolerances and toxicities: pharmacokinetic drug−drug interactions, particularly with ART drugs in patients coinfected with HIV, and patient adherence given the lengthy treatment regimens.[2] The most effective drugs in clinical use have been isoniazid, the first oral mycobactericidal drug, and rifampicin. The combined used of rifampicin and pyrazinamide shortened TB chemotherapy to 9 and 6 months, respectively.[3,4] Drug-resistant strains of Mtb fall into three main categories: multidrug resistant (MDR) TB, a form of TB caused by bacteria that do not respond to at least isoniazid and rifampicin, the two most powerful first-line anti-TB drugs; extremely drug resistant (XDR) TB, a form of MDR tuberculosis that responds to even fewer available medicines, including the most effective second-line anti-TB drugs; and totally drug resistant (TDR) TB, which describes strains of Mtb that are resistant to all available first- and second-line anti-TB drugs.[1,2,5]

MDR-TB is now a major problem globally and threatens the ability to treat and control TB infection. In 2015, an estimated 480 000 people developed MDR-TB, resulting in 190 000 deaths.[1] Treatment should be "individualized", based on drug susceptibility testing (DST). However, this is not always possible, and treatment is usually based on the pattern of drug resistance in the local geographical region. MDR-TB requires a longer treatment (18−24 months) with drugs that are more toxic and less efficacious. Worldwide, MDR-TB treatment success rates are as low as 50%.[5] XDR-TB requires third-line anti-TB drugs, which are expensive and are often associated with more severe side effects. The emergence of MDR-, XDR-, and TDR-TB strains has led to intensified research to identify new anti-TB drugs over the past decade.

Mycobacterium tuberculosis encodes 20 cytochrome P450 enzymes (CYPs or P450s). One of these is CYP121A1, which was shown to be essential for microbial viability.[6] CYP121A1 catalyzes the formation of an unusual intramolecular bond between carbon atoms in the *ortho*-positions of two tyrosine groups in the cyclodipeptide dicyclotyrosine (cYY), the natural substrate, to form the metabolite mycocyclosin. cYY interacts indirectly with the heme iron through water molecules (Figure 1A). Interestingly, this type of indirect binding mode was also observed in the crystal structure of CYP121A1 bound to the azole antifungal drug fluconazole.[7] The crystal structure of the CYP121A1/fluconazole complex, PDB 2IJ7, exhibits dual fluconazole conformations (I and II). In the indirect conformation (I), a triazole nitrogen of fluconazole binds to the heme iron via a distal water molecule that remains coordinated to the heme iron. However, in the direct conformation (II), the fluconazole binds through a triazole nitrogen directly to the heme iron (Figure 1B). While both binding modes are evident, the indirect binding (via water) mode appears predominant in this structure.[8]

The natural substrate cYY binds to the CYP121A1 active site without inducing any significant change in the P450 structure, consistent with it being a good substrate for the enzyme.[6] Through crystallization of ligand complexes, it was discovered that iodopyrazole binds with its pyrazole group in a channel between P450 helices F and G and "stacked" between Trp182 and Phe168 side chains. The iodine atom protrudes toward the active site and interacts with hydrophobic amino acids.[7] In designing potential new inhibitors of CYP121A1, we noted that "Y-shaped" molecules might provide a good "fit" within the P450 active site. This may be the result of a high conformational energy barrier necessary for binding to CYP121A1.

Using this observation to help design novel CYP121A1 inhibitors, our research explored the CYP121A1 binding and antimycobacterial activity of various "Y-shaped" biaryl pyrazole imidazole or triazole derivatives (Figure 2). Using different linkers between the hydrophobic biaryl pyrazole moiety (blue, Figure 2) and the heme binding azole group (red, Figure 2), the proximity of the heme binding moiety will be extended to determine if this has an effect on the indirect/direct binding of new ligands to the heme iron.

RESULTS AND DISCUSSION

Chemistry. The imidazole (**7**) or triazole (**8**) pyrazole compounds were obtained via a five-step synthetic route (Scheme 1) beginning with the preparation of the imines (**3**)

DOI: 10.1021/acs.jmedchem.7b01562
J. Med. Chem. 2017, 60, 10257−10267

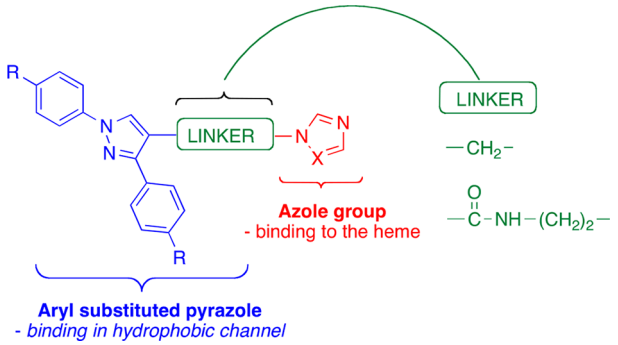

Figure 2. General structure of "Y-shaped" biaryl pyrazole, imidazole, and triazole derivatives showing different linkers.

by the reaction of acetophenones (**1**) with phenylhydrazine under acidic conditions.[9,10] The aldehydes (**4**) were prepared as previously described[9,10] by a Vilsmeier–Haack reaction of the imines (**3**). Reduction of the aldehydes (**4**) with $NaBH_4$ resulted in high yields of the corresponding alcohols (**5**), which were subsequently converted to the chlorides (**6**) by treatment with thionyl chloride in toluene at 115 °C for 2 h.[11] The chlorides were generally found to be unstable, so they were prepared immediately before use in the following step. Reaction of the chlorides (**6**) with either the potassium salt of imidazole or triazole, prepared in situ by treatment of imidazole or triazole with potassium carbonate in acetonitrile at 45 °C for 1 h, overnight at 70 °C, gave the required final imidazole (**7**) and triazole (**8**) pyrazole derivatives (Scheme 1).

The "extended" pyrazole compounds were prepared from the aldehydes (**4**). Oxidation to the carboxylic acids (**9**) was achieved by treatment of the aldehydes (**4**) with potassium permanganate (Scheme 2).[12] To prepare the aminoethylimidazole dihydrochloride salt (**12**), the corresponding 2-(2-(1*H*-imidazol-1-yl)ethyl)isoindoline-1,3-dione (**11**) was required. The isoindoline-1,3-dione was prepared by following the procedure of Popkov and Skvortsova,[13] which involved melted imidazole refluxed with bromoethylphthalamide (**10**) and potassium iodide, resulting in the desired product (**11**) in 49% yield after recrystallization from isopropanol. The isoindole-1,3-dione was then treated with hydrazine following the Ing–Manske procedure to give the required aminoethylimidazole dihydrochloride (**12**) in 82% yield (Scheme 2).

The final amides (**13**) were prepared by a carbonyldiimidazole (CDI) coupling reaction through the coupling of the carboxylic acids (**9**) with the free amine, generated in situ by the treatment of the aminoethylimidazole dihydrochloride salt (**13**) with triethylamine in DMF. The final amide derivatives (**13**) were obtained in low to moderate yields (Scheme 2).

CYP121A1 Ligand Binding Affinity. The CYP121A1 binding affinity (K_D) of the various compounds was determined by UV–vis optical titration. Results shown in Tables 1–3 reveal that most of the compounds show a red (type II) shift in the Soret peak position (Figure 3, for example **7b**), indicating that, in the solution state, most of these compounds coordinate either (i) directly to the CYP121A1 heme iron or (ii) indirectly to the heme iron through interstitial water molecule(s). Another possibility is (iii) that a ligand binding distant from

Scheme 1. Synthesis of Pyrazole Derivatives[a]

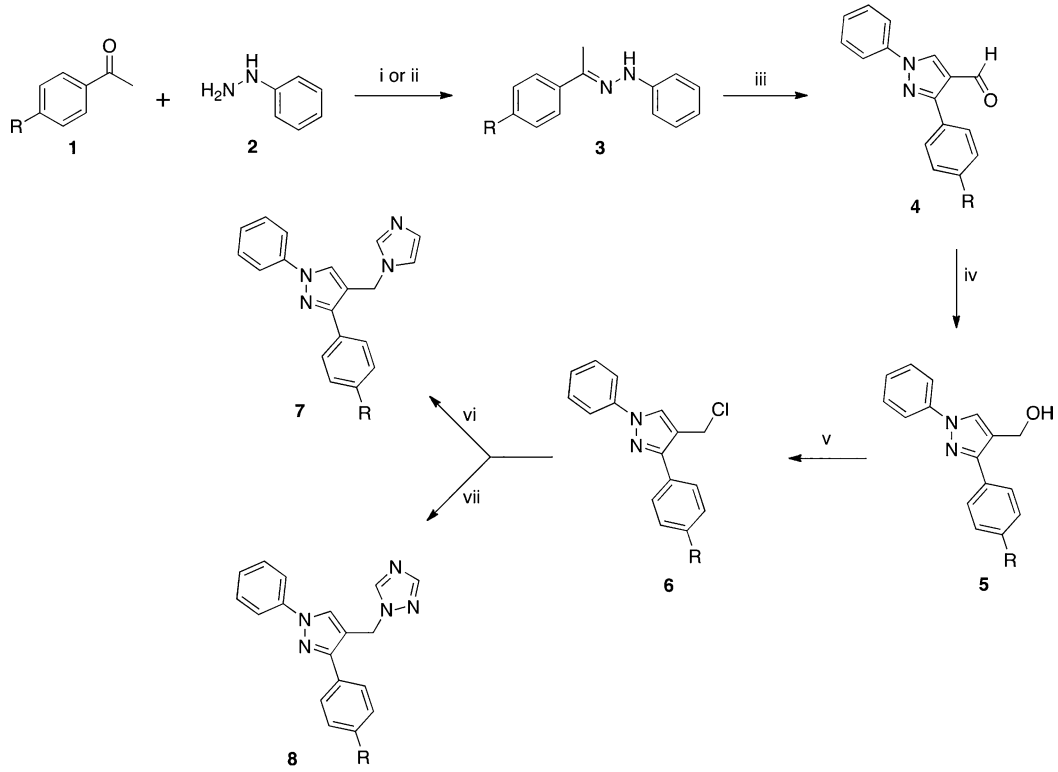

[a]Reagents and conditions: (i) AcOH, rt, 15 min; (ii) AcOH, EtOH, 80 °C, 1 h; (iii) $POCl_3$, DMF, 90 °C, 2 h; (iv) $NaBH_4$, EtOH, rt, 1 h; (v) $SOCl_2$, toluene, 115 °C, 2 h; (vi) imidazole, K_2CO_3, CH_3CN, 45 °C, 1 h then 70 °C, overnight; (vii) imidazole, K_2CO_3, CH_3CN, 45 °C, 1 h then 70 °C, overnight. [a, R = H; b, R = 4-F; c, R = 4-Cl; d, R = 4-CH_3; e, R = 4-OCH_3; f, R = 4-Br; g, R = 4-I; h, R = 4-CN].

DOI: 10.1021/acs.jmedchem.7b01562
J. Med. Chem. 2017, 60, 10257–10267

Scheme 2. Synthesis of Amide Derivatives[a]

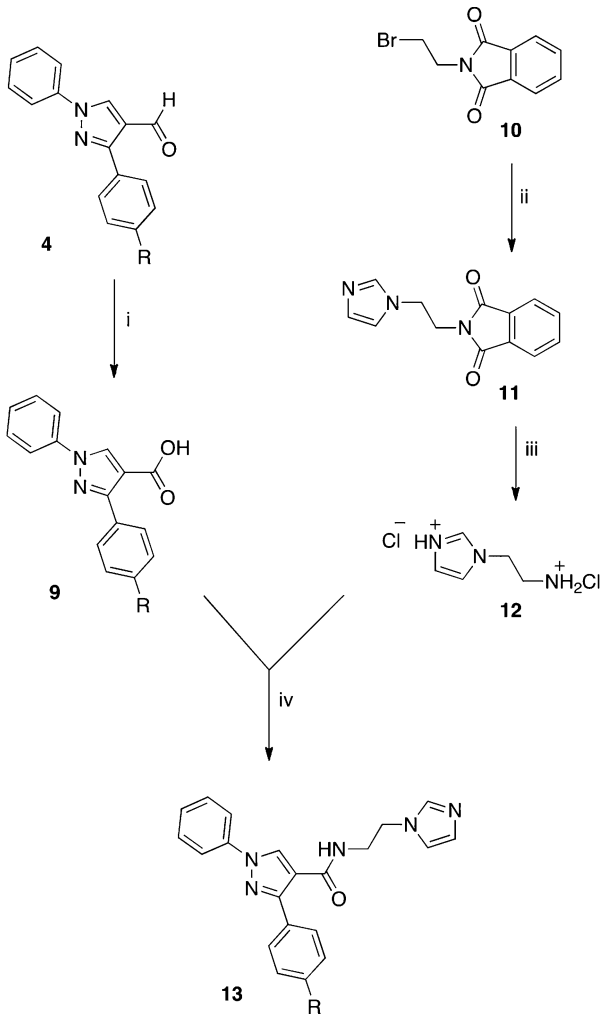

[a]Reagents and conditions: (i) $KMnO_4$, tBuOH/H_2O, 75 °C, 45 min; (ii) imidazole, 100 °C, 3 h, then toluene, 115 °C, 20 h; (iii) NH_2NH_2, EtOH, reflux, 4 h; (iv) CDI, DMF, 1 h then 12 h, Et_3N, DMF, rt, 20 h. [a, R = H; b, R = 4-F; c, R = 4-Cl; d, R = 4-CH_3; e, R = 4-OCH_3].

Table 1. K_D and MIC Values for Series 7 Against *M. tuberculosis* H37Rv

compound	R	K_D (μM)	Soret peak shift (nm)	MIC (μg/mL)
7a	H	2.63 ± 0.19	416–423.5	12.5
7b	F	4.16 ± 0.47	416–423.5	25
7c	Cl	7.42 ± 0.66	416–422	12.5
7d	CH_3	5.36 ± 0.59	416–421.5	12.5
7e	OCH_3	11.4 ± 0.9	416–421	25
7f	Br	19.5 ± 0.2	416–420	6.25
7g	I	13.6 ± 0.2	416–422	6.25
7h	CN	45.9 ± 0.6	416–418	100
fluconazole		8.6 ± 0.2		>100
clotrimazole		0.07 ± 0.01		20
cYY		5.82 ± 0.16		

the heme does not induce a heme spectral shift (but would block the active site).

Series **7** (imidazole derivatives) showed the highest affinity for CYP121A1, with compounds **7a–e** having K_D values <12 μM (K_D = 2.63 ± 0.19, 4.16 ± 0.47, 7.42 ± 0.66, 5.36 ± 0.59, and 11.35 ± 0.94 μM, respectively) (Table 1). The values are comparable with the K_D values for the azole drugs ketoconazole (imidazole) and fluconazole (triazole), which are 3.3 ± 0.3 and 8.6 ± 0.2 μM, respectively. Compounds **7a** and **7b** induce the most extensive Soret absorbance shifts (416–423.5 nm), suggesting that the CYP121A1 heme iron is predominantly coordinated by a direct imidazole nitrogen bond in these cases. Compounds **7c–h** show less extensive Soret red shifts for binding the CYP121A1 heme, suggesting that ligation modes in these cases may involve imidazole–nitrogen interactions with heme iron mediated through an interstitial water ligand and that these could occur to a greater (e.g., compounds **7f** and **7h**) or lesser (e.g., compounds **7c** and **7g**) extent. The smallest Soret shift occurs with compound **7h** (416–418 nm), and it is likely that the indirect coordination though the retained distal water on the heme iron is predominant in this case. However, alternative active site binding poses made by series **7** ligands that do not impact the heme iron or its distal water ligand cannot be ruled out at this stage, and this phenomenon could also provide explanations for the less extensive Soret shifts induced by a number of the series **7** molecules.

Series **8** (triazole derivatives) has affinities ranging from K_D = 35.6 ± 2.7 μM (compound **8b**) to 193 ± 21 μM (compound **8f**) (Table 2). Series **13** (pyrazole amide derivatives) had weaker affinities, with moderate K_D values between 290 and 400 μM (290 ± 27, 314 ± 43, and 394 ± 39 μM for compounds **13d**, **13e**, and **13a**, respectively). No evidence of binding was observed for the halogenated derivatives of this compound class (Table 3). As was also observed for series **7**, the extent of the CYP121A1 heme Soret shift observed at apparent saturation with the series **8** compounds varied considerably. In series **8**, a similar pattern of Soret shifts was observed to that seen with series **7**, with peak shifts as small as 416–417.5 nm (compound **8f**) and as large as 416–423 nm (compound **8b**). Again, we infer that the most extensive absorbance changes occur for those ligands that show predominantly direct coordination of heme iron through a triazole nitrogen (i.e., compounds **8a** and **8b**), while less extensive Soret shifts (i.e., compounds **8d** and **8f**) are likely indicative of either an indirect (through the heme distal water) coordination of the CYP121A1 heme iron or a possible result from mixed binding poses that include modes that do not influence the heme spectrum. For series **13**, ligand binding curves were obtained for the compounds **13a**, **13d**, and **13e**. However, the extents of the Soret band shift were modest (416–417.5/418 nm). Once again, these data suggest either indirect coordination of heme iron through an imidazole nitrogen or a combination of this type of ligand binding mode with other pose(s) that do not impact the heme spectrum.

Azole antifungal drugs (clotrimazole, econazole, fluconazole, ketoconazole, and miconazole) bind tightly to Mtb CYP121A1, inducing a Soret peak shift between 421 and 423.5 nm. The K_D values for clotrimazole, econazole, and miconazole are all <0.2 μM, indicating very tight binding, as determined from data fitting using the Morrison (quadratic) equation.[14]

MIC Determination Against *Mycobacterium tuberculosis*. The derivatives were screened against *M. tuberculosis* H37Rv by the REMA (Resazurin Microtiter Assay) method.[15] In the imidazole (**7**) and triazole (**8**) pyrazole series, the imidazoles (**7**) were generally more inhibitory to *M. tuberculosis* growth and displayed a better activity than the triazoles (**8**) (Tables 1 and 2), with the 4-bromo (**7f**) and 4-iodo (**7g**) derivatives displaying a good activity (MIC 6.25 μg/mL). All of

DOI: 10.1021/acs.jmedchem.7b01562
J. Med. Chem. 2017, 60, 10257–10267

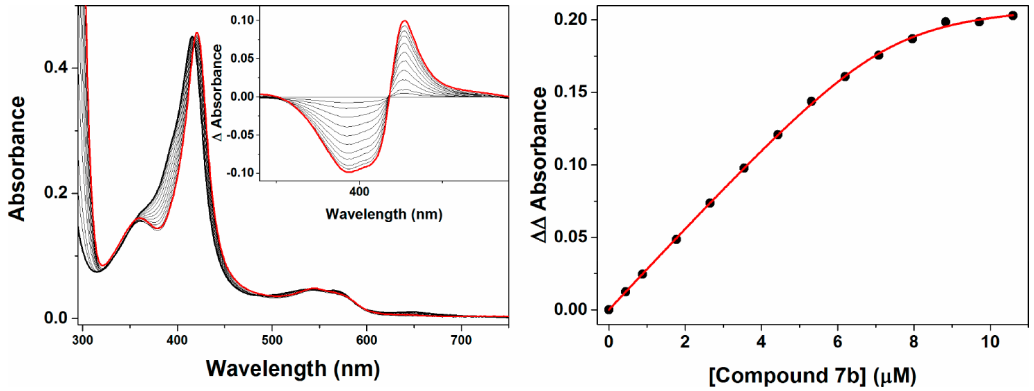

Figure 3. UV−Vis optical binding titration for compound **7b** binding to CYP121A1. The left-hand panel shows data from a compound **7b** titration with CYP121A1 (~4.7 μM) with the ligand-free spectrum as a thick black line, with the spectra following progressive additions of **7b** as thin solid lines, and with the final near-saturated protein spectrum shown as a thick red line. The inset shows an overlaid difference spectra generated by the subtraction of the starting spectrum from each consecutive ligand-bound spectrum collected in the titration. The right-hand panel shows a plot of compound **7b**-induced absorbance change, calculated as the difference between the peak and trough in the difference spectra in the left-hand panel, using the same wavelength pair (429 and 392 nm, respectively) throughout. Data were fitted using the Hill equation to give a **7b** K_D value of 4.16 ± 0.47 μM.

Table 2. K_D and MIC Values for Series 8 Against *M. tuberculosis* H37Rv

compound	R	K_D (μM)	Soret peak shift (nm)	MIC (μg/mL)
8a	H	73.5 ± 0.7	416−422	50
8b	F	35.6 ± 2.7	416−423	25
8c	Cl	83.8 ± 7.4	416−421	25
8d	CH_3	187 ± 13	416−418	>100
8e	OCH_3	96.5 ± 8.4	416−420	25
8f	Br	193 ± 21	416−417.5	25
8g	I		no binding	50
8h	CN		no binding	>100

Table 3. K_D and MIC Values for Series 13 Against *M. tuberculosis* H37Rv

compound	R	K_D (μM)	Soret peak shift (nm)	MIC (μg/mL)
13a	H	394 ± 39	416−417.5	>100
13b	F		no binding	>100
13c	Cl		no binding	>100
13d	CH_3	290 ± 27	416−417.5	>100
13e	OCH_3	314 ± 43	416−418	100

the imidazoles (**7**), with the exception of the 4-nitrile derivative (**7h**, MIC_{90} = 100 μg/mL), were significantly more active than the azole drug fluconazole. Compounds **7a−d**, **7f**, and **7g** are more active than clotrimazole (MIC_{90} = 20 μg/mL) (Table 1). The "extended" pyrazole compounds **13a−e** had little antimicrobial activity (MIC_{90} ≥ 100 μg/mL) (Table 3).

Molecular Modeling and Crystallography. The Molecular Operating Environment (MOE) program[16] was used to perform molecular docking and was found to closely replicate the position and binding interactions of cYY and fluconazole, as observed in the crystal structures PDB 3G5H and PDB 2IJ7, respectively.

The imidazole (**7**) and triazole (**8**) compounds were all found to interact with the heme through an interstitial water molecule via hydrogen-bonding interactions with Ser237, Gln 385, and Arg386 on one side of the structure, while on the other side of the structure interactions are through hydrophobic amino acid residues including Thr77, Val78, Val82, Val83, and Met86 (Figure 4A). The docking results were consistent with the type II binding indicated from the binding affinity assays. The only exception was the nitrile-substituted derivatives **7h** and **8h**. In both cases, the nitrile group interacted with Ala167 and Trp182 via interstitial water molecules, holding the compounds away from the active site with the imidazole/triazole ring positioned away from the heme group (Figure 4B).

The amide imidazole compounds (**13**) were positioned in a similar manner (Figure 4C) to **7** and **8**. However, whereas imidazole (**7**) and triazole (**8**) were consistently positioned within the active site, numerous conformations were observed for the amide imidazole series (**13**), possibly owing to their increased conformational flexibility, which may correlate with the moderate binding affinity observed.

Two compounds were successful cocrystallized with CYP121A1, **7b** and **7e** (Figure 5). However, the crystallized structures did not correlate with the binding affinity results as the imidazole group was positioned away from the heme group, and in both cases, the compounds were located in positions too far away to form direct or indirect binding interactions with the heme iron. However, the observed binding poses of **7b** and **7e** are similar, and both clearly result in effective blockage of the active site and thus result in inhibition of binding of the cYY substrate. These data illustrate how different P450 ligand binding modes can be adopted by molecules bound to proteins in the solution state or in the more constrained environment of protein crystals. In the case of the compound series investigated in this study, there is clear evidence from structural, molecular modeling and UV−visible ligand titration studies for the adoption of binding modes that involve direct or indirect (via the distal water ligand) coordination of the heme iron by imidazole or triazole nitrogens, as well as for modes in which the bound ligands are distant from the heme and are unlikely to influence the CYP121A1 heme spectrum.

CONCLUSION

The data presented demonstrate the successful binding to CYP121A1 of a range of different compounds inspired by the structure of CYP121A1's natural substrate (the cyclic dipeptide cYY). Series **7** produced the most effective antimycobacterial agents with the tightest binding constants and with K_D values

DOI: 10.1021/acs.jmedchem.7b01562
J. Med. Chem. 2017, 60, 10257−10267

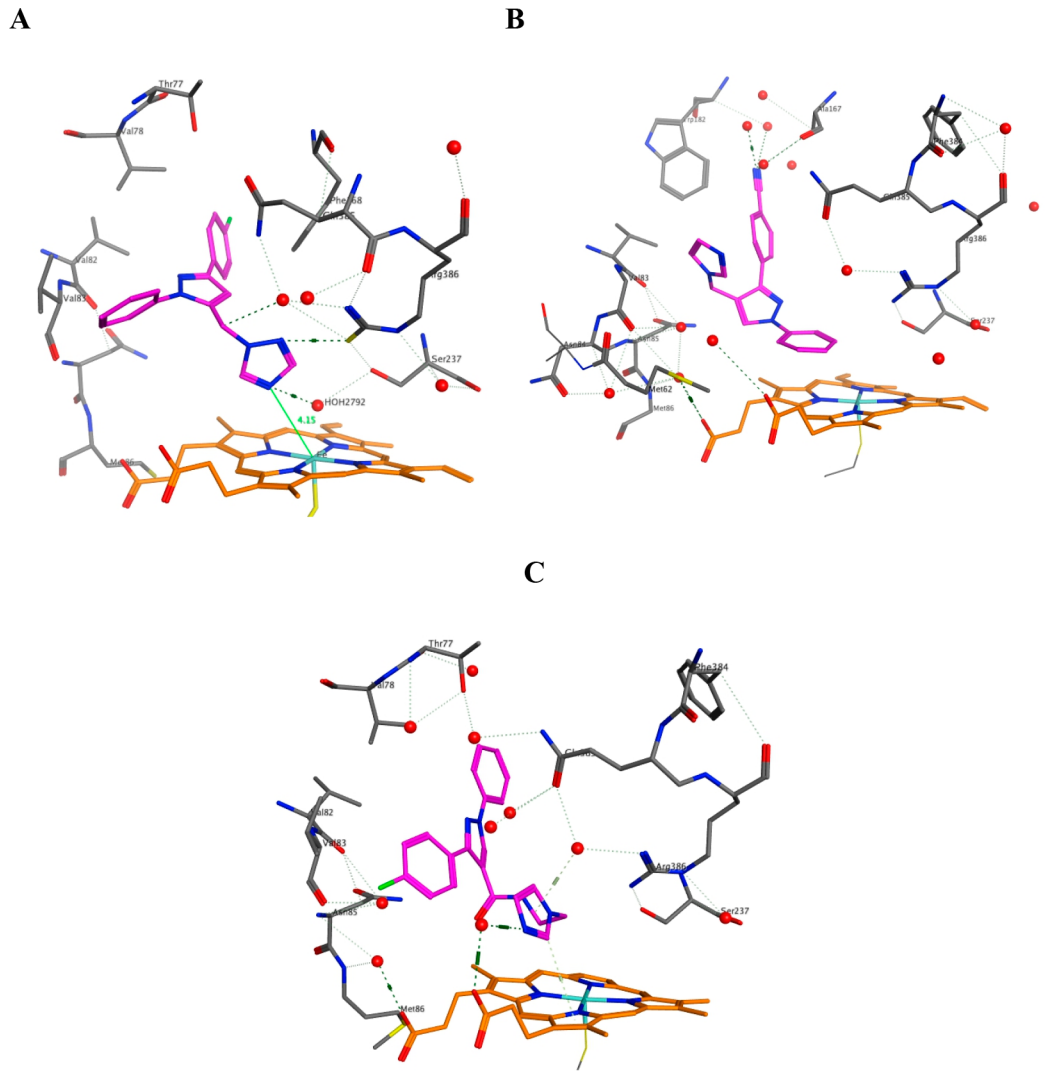

Figure 4. Molecular modeling of selected compounds. (A) The triazole group of **8b** interacts with the heme indirectly via an interstitial water molecule and binds in a similar conformation, and with the same key amino acids, as that observed for cYY and fluconazole. (B) The nitrile derivative **7h** binds in a different conformation with the nitrile bound to water molecules and held in a position further away from the heme active site. (C) The amide imidazole **13b** also interacts with the heme via an interstitial water molecule, but its greater flexibility also resulted in various other conformations.

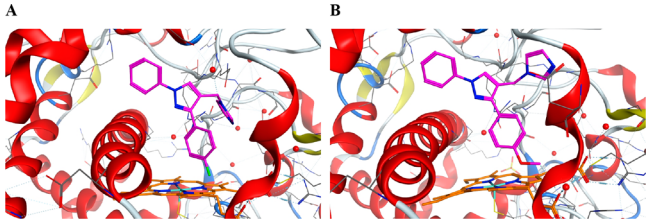

Figure 5. X-ray crystal structures of (A) **7b** and (B) **7e** binding to CYP121A1.

for the eight compounds in this series in the range between 2.63 and 45.9 μM, with an average (mean) K_D value of ~13.7 μM. The series **7** compounds with the best MIC values were those with bromo (**7f**) and iodo (**7g**) substituents (MIC = 6.25 μg/mL); the Hansch analysis suggested that increased lipophilicity (Figure 6) may correlate with improved anti-mycobacterial activity in this series, possibly through facilitating increased drug uptake across the Mtb lipid-rich cell wall (Table 1).

The 4-nitrile derivative **7h** is a relatively weak binder (K_D = 45.9 μM), a property which may be explained from molecular docking (Figure 4B) where the nitrile interacts with Ala167 and Trp182 via interstitial water molecules, holding the compound at a distance too far from the active site to attain indirect or direct interaction with the heme.

From the antimicrobial MIC data, it is clear that extending the "linker" region of the pyrazole derivatives from $-CH_2-$ (series **7** and **8**) to $-C(O)NH-(CH_2)_2-$ (series **13**) does not translate to improved MIC values. Computational docking studies suggested that these extended compounds (series **13**) were able to interact with the heme indirectly and fit within the hydrophobic CYP121A1 pocket. However, only moderate K_D values between 290 and 400 μM were observed for compounds **13d**, **13e**, and **13a**, respectively, with only partial type II heme shifts (416–417.5/418 nm). There was also no evidence of binding for halogenated derivatives of this compound class.

DOI: 10.1021/acs.jmedchem.7b01562
J. Med. Chem. 2017, 60, 10257–10267

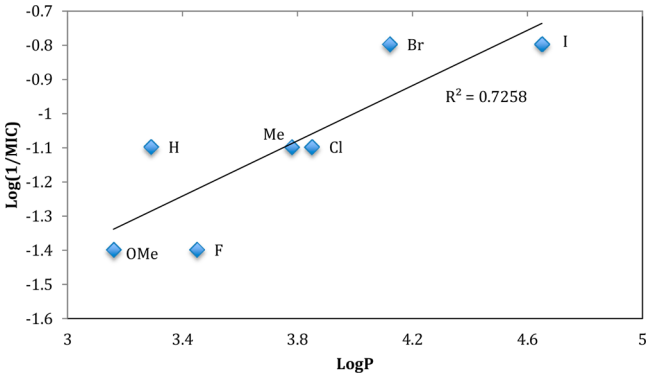

Figure 6. Hansch analysis illustrating correlation between MIC and calculated log P[17] values for the imidazole compounds (**7**). (Nitrile **7h** is excluded as an outlier.)

EXPERIMENTAL SECTION

General Procedures. All reagents and solvents were of general purpose or analytical grade and purchased from Sigma-Aldrich Ltd., Fisher Scientific, Fluka, and Acros. ^{1}H and ^{13}C NMR spectra were recorded with a Bruker Avance DPX500 spectrometer operating at 500 and 125 MHz, with Me_4Si as an internal standard. Mass spectra (HRMS) were determined by the EPSRC mass spectrometry center (Swansea, UK). Elemental analysis was performed by MEDAC Ltd. (Chobham, Surrey, UK). Flash column chromatography was performed with silica gel 60 (230−400 mesh) (Merck), and TLC was carried out on precoated silica plates (kiesel gel 60 F_{254}, BDH). Compounds were visualized by illumination under UV light (254 nm) or by the use of vanillin stain followed by heating. Melting points were determined on an electrothermal instrument and were uncorrected. All solvents were dried prior to use and stored over 4 Å molecular sieves, under nitrogen. All of the compounds were ≥95% pure.

The imines (**3**), aldehydes (**4**), alcohols (**5**), chlorides (**6**), carboxylic acids (**9**), and 1-(2-ammonioethyl)-1*H*-imidazol-3-ium chloride (**12**) were prepared as previously described.[9−13] All compounds were more than 95% pure.

*General Method for the Preparation of Imidazole and Triazole Derivatives **7** and **8**.* To a stirred suspension of K_2CO_3 (3 mmol) in dry acetonitrile (20 mL) was added imidazole (3 mmol) or triazole (3 mmol). The reaction mixture was refluxed at 45 °C for 1 h. After cooling the mixture to room temperature, the chloromethyl pyrazole compound (**6**) (0.76 mmol) was added, and the reaction mixture refluxed at 70 °C overnight. The solvent was evaporated under reduced pressure, and the resulting mixture was diluted with EtOAc (50 mL) and washed with H_2O (3 × 20 mL). The EtOAc layer was dried ($MgSO_4$) and evaporated under reduced pressure to give the crude imidazole (**7**) or triazole (**8**), which was further purified by recrystallization.

*(1,3-Diphenyl)-4-((1,3-imidazol-1-yl)methyl)-1H-pyrazole (**7a**).* Compound **7a** was prepared from 4-(chloromethyl)-1,3-diphenyl-*1H*-pyrazole (**6a**) (0.35 g, 1.3 mmol) and was obtained as a yellow crystalline solid after recrystallization from methanol, yield 0.12 g (32%). Mp 124−128 °C. TLC (3:1 petroleum ether/EtOAc), R_f = 0.06. ^{1}H NMR ($CDCl_3$): δ 7.85 (s, 1H, pyrazole), 7.74 (d, J = 7.7 Hz, 2H, triazole), 7.68 (s, 1H, Ar), 7.61 (d, J = 7.0 Hz, 2H, Ar), 7.42−7.50 (m, 5H, Ar), 7.33 (t, J = 7.5 Hz, 1H, Ar), 7.12 (s, 1H, Ar), 6.96 (s, 1H, Ar), 5.26 (s, 2H, CH_2). ^{13}C NMR ($CDCl_3$): δ 151.4, 116.2 (2 × pyrazole), 139.6, 132.4 (2 × Ar), 136.9, 129.5, 129.3, 128.9, 128.6, 127.9, 127.7, 126.4, 119.1, 119.0 (12 × CH, Ar), 41.9 (CH_2). Anal. Calcd for $C_{19}H_{16}N_4$ (300.36): C, 75.98; H, 5.37; N, 18.64. Found: C, 76.10; H, 5.39; N, 18.58.

*4-((1H-Imidazol-1-yl)methyl)-3-(4-fluorophenyl)-1-phenyl-1H-pyrazole (**7b**).* Compound **7b** was prepared from 4-(chloromethyl)-3-(4-fluorophenyl)-1-phenyl-*1H*-pyrazole (**6b**) (0.22 g, 0.76 mmol) and was obtained as a yellow crystalline solid after recrystallization from EtOH/H_2O 1:1 v/v, yield 0.07 g (29%). Mp 128−130 °C. TLC (3:1 petroleum ether/EtOAc), R_f = 0.06. ^{1}H NMR ($CDCl_3$): δ 7.89 (s, 1H, pyrazole), 7.78 (s, 1H, Ar), 7.73 (d, J = 7.8 Hz, 2H, Ar), 7.55−7.58 (m, 2H, Ar), 7.49 (t, J = 7.7 Hz, 2H, Ar), 7.34 (t, J = 7.5 Hz, 1H, Ar), 7.13−7.18 (m, 3H, Ar), 6.95 (s, 1H, Ar), 5.25 (s, 2H, CH_2). ^{13}C NMR ($CDCl_3$): δ 164.0, 150.6, 139.5 (3 × C, Ar), 162.0, 128.5 (2 × C, pyrazole), 136.8, 129.7, 129.6, 128.9, 128.0, 127.0, 117.1, 117.0, 116.0, 115.8 (13 × CH, Ar), 41.9 (CH_2). Anal. Calcd for $C_{19}H_{15}FN_4$ (318.35): C, 71.68; H, 4.75; N, 17.60. Found: C, 71.51; H, 4.98; N, 17.62.

*4-((1H-Imidazol-1-yl)methyl)-3-(4-chlorophenyl)-1-phenyl-1H-pyrazole (**7c**).* Compound **7c** was prepared from 4-(chloromethyl)-3-(4-chlorophenyl)-1-phenyl-*1H*-pyrazole (**6c**) (0.91 g, 3 mmol) and was obtained as a yellow crystalline solid after recrystallization from ethanol, yield 0.52 g (52%). Mp 155−158 °C. TLC (3:1 petroleum ether/EtOAc), R_f = 0.05. ^{1}H NMR ($CDCl_3$): δ 7.88 (s, 1H, pyrazole), 7.78 (s, 1H, Ar), 7.73 (d, J = 8.4 Hz, 2H, Ar), 7.54 (d, J = 8.0 Hz, 2H, Ar), 7.49 (d, J = 7.6 Hz, 2H, Ar), 7.45 (d, J = 8.1 Hz, 2H, Ar), 7.35 (t, J = 7.4 Hz, 1H Ar), 7.14 (s, 1H, Ar), 6.96 (s, 1H, Ar), 5.26 (s, 2H, CH_2). ^{13}C NMR ($CDCl_3$): δ 150.3, 116.0 (2 × C, pyrazole), 139.5, 134.6, 130.8 (3 × C, Ar), 136.8, 129.6, 129.1, 129.0, 128.1, 127.1, 119.1, 119.0 (12 × CH, Ar), 41.9 (CH_2). Anal. Calcd for $C_{19}H_{15}ClN_4$ (334.80): C, 68.16; H, 4.52; N, 16.73. Found: C, 68.09; H, 4.17; N, 16.58.

*4-((1H-Imidazol-1-yl)methyl)-1-phenyl-3-(p-tolyl)-1H-pyrazole (**7d**).* Compound **7d** was prepared from 4-(chloromethyl)-1-phenyl-3-(*p*-tolyl)-*1H*-pyrazole (**6d**) (0.35 g, 1.24 mmol) and was obtained as a yellow-orange crystalline solid after recrystallization from EtOH/H_2O 1:1 v/v, yield 0.065 g (17%). Mp 145−148 °C. TLC (3:1 petroleum ether/EtOAc), R_f = 0.05. ^{1}H NMR ($CDCl_3$): δ 7.87 (s, 1H, pyrazole), 7.8 (s, 1H, Ar), 7.74 (d, J = 8.3 Hz, 2H, Ar), 7.48−7.50 (m, 4H, Ar), 7.28−7.34 (m, 4H, Ar), 7.13 (s, 1H, Ar), 6.95 (s, 1H, Ar), 5.27 (s, 2H, CH_2), 2.43 (s, 3H, CH_3). ^{13}C NMR ($CDCl_3$): δ 151.5, 115.9 (2 × C, pyrazole), 139.7, 138.5, 129.4 (3 × C, Ar), 136.8, 129.6, 129.5, 128.6, 127.8, 127.7, 126.8, 119.1 (13 × CH, Ar), 42.0 (CH_2), 21.3 (CH_3). Anal. Calcd for $C_{20}H_{18}N_4$ (314.38): C, 76.41; H, 5.77; N, 17.81. Found: C, 76.40; H, 5.79; N, 17.77.

*4-((1H-Imidazol-1-yl)methyl)-3-(4-methoxyphenyl)-1-phenyl-1H-pyrazole (**7e**).* Compound **7e** was prepared from 4-(chlorophenyl)-3-(4-methoxyphenyl)-1-phenyl-*1H*-pyrazole (**6e**) (0.88g, 2.9 mmol) and was obtained as a white crystalline solid after recrystallization from EtOH/H_2O 1:1 v/v, yield 0.42 g (43%). Mp 102−106 °C. TLC (3:1 petroleum ether/EtOAc), R_f = 0.05. ^{1}H NMR ($CDCl_3$): δ 7.89 (s, 1H, pyrazole), 7.85 (s, 1H, Ar), 7.74 (d, J = 7.6 Hz, 2H, Ar), 7.52 (d, J = 8.8 Hz, 2H, Ar), 7.48 (d, J = 7.5 Hz, 2H, Ar), 7.32 (t, J = 7.5 Hz, 1H, Ar), 7.14 (s, 1H, Ar), 7.01 (d, J = 8.8 Hz, 2H, Ar), 6.96 (s, 1H, Ar), 5.27 (s, 2H, CH_2), 3.88 (s, 3H, OCH_3). ^{13}C NMR ($CDCl_3$): δ 159.9, 139.7, 124.8 (3 × C, Ar), 151.4, 115.6 (2 × C, pyrazole), 136.8, 129.5, 129.1, 128.5, 127.5, 126.8, 119.0, 114.4 (13 × CH, Ar), 55.4 (CH_3), 42.1 (CH_2). Anal. Calcd for $C_{20}H_{18}N_4O$ (330.39): C, 71.68; H, 4.75; N, 17.60. Found: C, 71.66; H, 4.76; N, 17.54.

*4-((1H-Imidazole-1-yl)methyl)-3-(4-bromophenyl)-1-phenyl-1H-pyrazole (**7f**).* Compound **7f** was prepared from (4-(chloromethyl)-3-(4-bromophenyl)-1-phenyl-1*H*-pyrazole) (**6f**) (0.75 g, 2.2 mmol) and was obtained as a white crystalline solid after recrystallization from EtOH/H_2O 1:1 v/v, yield 0.45 g (56%). Mp 161−163 °C. TLC (9:1 CH_2Cl_2/MeOH), R_f = 0.83. ^{1}H NMR ($CDCl_3$): δ 8.60 (s, 1H, pyrazole), 8.15 (s, 1H, imidazole), 7.75 (d, J = 7.6 Hz, 2H, Ar), 7.60 (d, J = 8.4 Hz, 2H, Ar), 7.5−7.47 (m, 4H, Ar), 7.35 (t, J = 7.4 Hz, 1H, Ar), 7.20 (s, 1H, imidazole), 6.90 (s, 1H, imidazole), 5.43 (s, 2H, CH_2). ^{13}C NMR ($CDCl_3$): δ 150.2 (C, pyrazole), 139.5 (C, Ar), 137.0 (CH, imidazole), 132.0 (2 × CH, Ar), 131.3 (C, Ar), 130.0 (CH, Ar), 129.6 (C, Ar), 129.3 (CH, imidazole), 127.9 (2 × CH, Ar), 127.1 (2 × CH, Ar), 122.8 (CH, pyrazole), 119.1 (2 × CH, Ar), 118.9 (CH, imidazole), 116.4 (C, pyrazole), 41.7 (CH_2). Anal. Calcd for $C_{19}H_{15}N_4Br$ (379.25): C, 60.17; H, 3.99; N, 14.77. Found: C, 59.92; H, 4.02; N, 14.67.

*4-((1H-Imidazole-1-yl)methyl)-3-(4-iodophenyl)-1-phenyl-1H-pyrazole (**7g**).* Compound **7g** was prepared from (4-(chloromethyl)-3-(4-iodophenyl)-1-phenyl-1*H*-pyrazole) (**6g**) (0.75 g, 1.9 mmol) and was obtained as a pale yellow crystalline solid after recrystallization

DOI: 10.1021/acs.jmedchem.7b01562
J. Med. Chem. 2017, 60, 10257−10267

from EtOH/H_2O 1:1 v/v, yield 0.45 g (55%). Mp 169−173 °C. TLC (3:2 petroleum ether/EtOAc), R_f = 0.08. ^{1}H NMR ($CDCl_3$): δ 8.10 (s, 1H, pyrazole), 7.90 (s, 1H, imidazole), 7.80 (d, J = 8.5 Hz, 2H, Ar), 7.74 (m, 3H, Ar), 7.16 (s, 1H, imidazole), 6.95 (s, 1H, imidazole), 5.32 (s, 2H, CH_2). ^{13}C NMR ($CDCl_3$): δ 150.3 (C, pyrazole), 139.5 (C, Ar), 138.0 (2 × CH, Ar), 137.0 (CH, imidazole), 131.9 (C, Ar), 130.0 (CH, Ar), 129.6 (CH, imidazole), 129.5 (2 × CH, Ar), 127.9 (2 × CH, Ar), 127.1 (CH, pyrazole), 119.1 (2 × CH, Ar), 118.9 (CH, imidazole), 116.4 (C, pyrazole), 94.4 (C, C−I), 41.7 (CH_2). Anal. Calcd for $C_{19}H_{15}N_4I$ (426.25): C, 53.54; H, 3.55; N, 13.14. Found: C, 53.74; H, 3.23; N, 13.15.

*4-(4-((1H-Imidazol-1-yl)methyl)-1-phenyl-1H-pyrazol-3-yl)-benzonitrile (**7h**).* Compound **7h** was prepared from 4-(4-(chloromethyl)-1-phenyl-1*H*-pyrazol-3-yl)benzonitrile (**6h**) (0.75 g, 2.5 mmol) and was obtained as a pale yellow crystalline solid after recrystallization from EtOH/H_2O 1:1 v/v, yield 0.46 g (57%). Mp 197−200 °C. TLC (9:1 CH_2Cl_2/MeOH), R_f = 0.63. ^{1}H NMR ($CDCl_3$): δ 7.83 (s, 1H, pyrazole), 7.76−7.72 (m, 6H, Ar), 7.58 (s, 1H, imidazole), 7.50 (t, J = 8.0 Hz, 2H, Ar), 7.40 (t, J = 7.4 Hz, 1H, Ar), 7.14 (s, 1H, imidazole), 6.90 (s, 1H, imidazole), 5.27 (s, 2H, CH_2). ^{13}C NMR ($CDCl_3$): δ 149.1 (C, pyrazole), 139.3 (C, Ar), 137.0 (CH, imidazole), 132.8 (CH, imidazole), 132.6 (2 × CH, Ar), 130.2 (2 × CH, Ar), 129.7 (CH, imidazole), 128.3 (2 × CH, Ar), 128.1 (CH, pyrazole), 127.4 (2 × CH, Ar), 119.2 (CN), 118.8 (C, Ar), 116.8 (C, pyrazole), 112.0 (C, Ar), 41.7 (CH_2). Anal. Calcd for $C_{20}H_{15}N_5$ (325.37): C, 73.83; H, 4.65; N, 21.52. Found: C, 73.76; H, 4.69; N, 21.51.

*1-((1,3-Diphenyl-1H-pyrazol-4-yl)methyl)-1H-[1,2,4]triazole (**8a**).* Compound **8a** was prepared from 4-(chloromethyl)-1,3-diphenyl-1*H*-pyrazole (**6a**) (0.40 g, 1.5 mmol) and was obtained as a light yellow crystalline solid after recrystallization from methanol, yield 0.115 g (26%). Mp 101−104 °C. TLC (3:1 petroleum ether/EtOAc), R_f = 0.06. ^{1}H NMR ($CDCl_3$): δ 8.29 (s, 1H, pyrazole), 8.07 (m, 2H, Ar), 7.77 (d, J = 7.7 Hz, 2H, Ar), 7.65 (d, J = 7.0 Hz, 2H, Ar), 7.42−7.50 (m, 5H, Ar), 7.34 (t, J = 7.5 Hz, 1H, Ar), 5.50 (s, 2H, CH_2). ^{13}C NMR ($CDCl_3$): δ 151.7, 114.1 (2 × C, pyrazole), 139.6, 132.1 (2 × C, Ar), 151.1, 142.6, 129.5, 128.9, 128.7, 128.6, 128.0, 127.0, 119.2 (13 × CH, Ar), 44.7 (CH_2). Anal. Calcd for $C_{19}H_{15}N_5$ (301.35): C, 71.74; H, 5.02; N, 23.23. Found: C, 71.97; H, 5.06; N, 23.35.

*1-((3-(4-Fluorophenyl)-1-phenyl-1H-pyrazole-4-yl)methyl)-1H-1,2,4-triazole (**8b**).* Compound **8b** was prepared from 4-(chloromethyl)-3-(4-fluorophenyl)-1-phenyl-1*H*-pyrazole (**6b**) (0.15 g, 0.52 mmol) and was obtained as a pale yellow crystalline solid after recrystallization from EtOH/H_2O 1:1 v/v, yield 0.039 g (24%). Mp 114−118 °C. TLC (3:1 petroleum ether/EtOAc), R_f = 0.06. ^{1}H NMR ($CDCl_3$): δ 8.09 (s, 1H, pyrazole), 8.03 (d, J = 7.7 Hz, 2H, triazole), 7.75 (d, J = 7.6 Hz, 2H, Ar), 7.61−7.64 (m, 2H, Ar), 7.49 (t, J = 7.7 Hz, 2H, Ar), 7.35 (t, J = 7.4 Hz, 1H, Ar), 7.17 (t, J = 8.7 Hz, 2H, Ar), 5.45 (s, 2H, CH_2). ^{13}C NMR ($CDCl_3$): δ 164.0, 150.8, 139.5 (3 × C, Ar), 150.8, 114.2 (2 × C, pyrazole), 152.1, 142.7, 129.8, 129.7, 129.5, 128.5, 127.1, 119.2, 116.0, 115.8 (12 × CH, Ar), 44.4 (CH_2). Anal. Calcd for $C_{18}H_{14}FN_5$ (319.34): C, 67.70; H, 4.42; N, 21.92. Found: C, 67.98; H, 4.00; N, 22.05.

*1-((3-(4-Chlorophenyl)-1-phenyl-1H-pyrazole-4-yl)methyl)-1H-1,2,4-triazole (**8c**).* Compound **8c** was prepared from 4-(chloromethyl)-3-(4-chlorophenyl)-1-phenyl-1*H*-pyrazole (**6c**) (0.61 g, 2 mmol) and was obtained as a pale yellow crystalline solid after recrystallization from ethanol, yield 0.27 g (40%). Mp 119−122 °C. TLC (3:1 petroleum ether/EtOAc), R_f = 0.05. ^{1}H NMR ($CDCl_3$): δ 8.10 (s, 1H, pyrazole), 8.02 (s, 2H, triazole), 7.74 (d, J = 7.8 Hz, 2H, Ar), 7.60 (d, J = 8.5 Hz, 2H, Ar), 7.44−7.51 (m, 4H, Ar), 7.35 (t, J = 7.5 Hz, 1H, Ar), 5.55 (s, 2H, CH_2). ^{13}C NMR ($CDCl_3$): δ 150.5, 114.4 (2 × C, pyrazole), 139.5, 134.7, 120.7 (3 × C, Ar), 150.2, 142.7, 129.6, 129.2, 129.1, 128.6, 127.1, 119.2 (12 × CH, Ar), 44.3 (CH_2). Anal. Calcd for $C_{18}H_{14}ClN_5$ (335.79): C, 64.38; H, 4.20; N, 20.85. Found: C, 64.63; H, 3.81; N, 21.14.

*1((1-Phenyl-3-(p-tolyl)-1H-pyrazol-4-yl)methyl)-1H-1,2,4-triazole (**8d**).* Compound **8d** was prepared from 4-(chloromethyl)-1-phenyl-3-(*p*-tolyl)-1*H*-pyrazole (**6d**) (0.35 g, 1.24 mmol) and was obtained as a yellow-orange crystalline solid after recrystallization from EtOH/H_2O 1:1 v/v, yield 0.11 g (29%). Mp 128−130 °C. TLC (3:1 petroleum ether/EtOAc), R_f = 0.14. ^{1}H NMR ($CDCl_3$): δ 8.14 (s, 1H, pyrazole), 8.04 (d, J = 5.6 Hz, 2H, Ar), 7.76 (d, J = 8.1 Hz, 2H, Ar), 7.52 (d, J = 7.9 Hz, 2H, Ar), 7.48 (t, J = 7.8 Hz, 2H, Ar), 7.33 (t, J = 7.2 Hz, 1H, Ar), 7.28−7.30 (m, 2H, Ar), 5.47 (s, 2H, CH_2), 2.43 (s, 3H, OCH_3). ^{13}C NMR ($CDCl_3$): δ 151.8, 114.1 (2 × C, pyrazole), 139.7, 138.6, 129.3 (3 × C, Ar), 151.6, 142.2, 129.6, 129.5, 128.4, 127.8, 126.9, 119.1 (12 × CH, Ar), 44.6 (CH_2), 21.3 (CH_3). Anal. Calcd for $C_{19}H_{17}N_5$ (315.37): C, 72.36; H, 5.43; N, 22.20. Found: C, 72.43; H, 5.43; N, 22.41.

*1-((3-(4-Methoxyphenyl)-1-phenyl-1H-pyrazol-4-yl)methyl)-1H-1,2,4-triazole (**8e**).* Compound **8e** was prepared from 4-(chlorophenyl)-3-(4-methoxyphenyl)-1-phenyl-1*H*-pyrazole (**6e**) (0.45 g, 1.5 mmol) and was obtained as an orange crystalline solid after recrystallization from EtOH/H_2O 1:1 v/v, yield 0.21 g (43%). Mp 106−108 °C. TLC (3:1 petroleum ether/EtOAc), R_f = 0.05. ^{1}H NMR ($CDCl_3$): δ 8.21 (s, 1H, pyrazole), 8.05 (d, J = 7.7 Hz, 2H, Ar), 7.76 (d, J = 8.0 Hz, 2H, Ar), 7.57 (d, J = 8.7 Hz, 2H, Ar), 7.48 (d, J = 8.0 Hz, 2H, Ar), 7.33 (t, J = 7.4 Hz, 1H, Ar), 7.01 (d, J = 8.7 Hz, 2H, Ar), 5.47 (s, 2H, CH_2), 3.88 (s, 3H, OCH_3). ^{13}C NMR ($CDCl_3$): δ 160.0, 139.7, 124.7 (3 × C, Ar), 151.6, 114.0 (2 × C, pyrazole), 151.9, 142.7, 129.6, 129.5, 129.2, 128.4, 126.8, 119.2, 114.2 (12 × CH, Ar), 55.4 (CH_3), 44.5 (CH_2). Anal. Calcd for $C_{19}H_{17}N_5O$ (331.37): C, 68.87; H, 5.17; N, 21.12. Found: C, 68.87; H, 4.87; N, 21.15.

*1-((3-(4-Bromophenyl)-1-phenyl-1H-pyrazol-4-yl)methyl)-1H-1,2,4-triazole (**8f**).* Compound **8f** was prepared from (4-(chloromethyl)-3-(4-bromophenyl)-1-phenyl-1*H*-pyrazole) (**6f**) (0.7 g, 2 mmol) and was obtained as a white crystalline solid after recrystallization from EtOH/H_2O 1:1 v/v, yield 0.36 g (47%). Mp 144−146 °C. TLC (9:1 CH_2Cl_2/MeOH), R_f = 0.68. ^{1}H NMR ($CDCl_3$): δ 8.04 (s, 1H, pyrazole), 8.02 (s, 2H, triazole), 7.74 (dd, J = 1.1, 8.7 Hz, 2H, Ar), 7.6 (dd, J = 1.9, 6.6 Hz, 2H, Ar), 7.54 (s, 1H, Ar), 7.52−7.48 (m, 2H, Ar), 7.35 (t, J = 7.4 Hz, 1H, Ar), 5.45 (s, 2H, CH_2). ^{13}C NMR ($CDCl_3$): δ 152.4 (CH, triazole), 150.5 (C, pyrazole), 142.8 (CH, triazole), 139.5 (C, Ar), 132.2 (2 × CH, Ar), 129.7 (2 × CH, Ar), 129.6 (CH, Ar), 129.4 (2 × CH, Ar), 129.3 (CH, Ar), 128.6 (CH, pyrazole), 128.0 (C, pyrazole), 127.2 (2 × CH, Ar), 114.4 (C, Ar), 44.3 (CH_2). Anal. Calcd for $C_{18}H_{14}N_5Br$ (380.24): C, 56.86; H, 3.71; N, 18.42. Found: C, 56.48; H, 3.99; N, 18.43.

*1-((3-(4-Iodophenyl)-1-phenyl-1H-pyrazol-4-yl)methyl)-1H-1,2,4-triazole (**8g**).* Compound **8g** was prepared from (4-(chloromethyl)-3-(4-iodophenyl)-1-phenyl-1*H*-pyrazole) (**6g**) (0.8 g, 2 mmol) and was obtained as a white crystalline solid after recrystallization from EtOH/H_2O 1:1 v/v, yield 0.4 g (46%). Mp 151−155 °C. TLC (9:1 CH_2Cl_2/MeOH), R_f = 0.13. ^{1}H NMR ($CDCl_3$): δ 8.03 (s, 1H, pyrazole), 8.01 (s, 2H, triazole), 7.82 (dd, J = 1.8, 6.6 Hz, Ar), 7.74 (dd, J = 1.2, 8.7 Hz, 2H, Ar), 7.50 (t, J = 8.0 Hz, 2H, Ar), 7.40 (d, J = 8.4 Hz, 2H, Ar), 7.35 (t, J = 7.4 Hz, 1H, Ar), 5.45 (s, 2H, CH_2). ^{13}C NMR ($CDCl_3$): δ 152.4 (CH, triazole), 150.6 (C, pyrazole), 142.8 (CH, triazole), 139.5 (C, Ar), 138.0 (2 × CH, Ar), 131.7 (CH, Ar), 129.6 (2 × CH, Ar), 129.4 (2 × CH, Ar), 128.7 (CH, Ar), 127.4 (CH, pyrazole), 119.2 (2 × CH, Ar), 114.4 (C, pyrazole), 94.6 (C−I), 44.3 (CH_2). Anal. Calcd for $C_{18}H_{14}N_5I$ (427.24): C, 50.60; H, 3.30; N, 16.39. Found: C, 50.87; H, 3.27; N, 16.38.

*4-(4-((1H-Triazol-1-yl)methyl)-1-phenyl-1H-pyrazol-3-yl)-benzonitrile (**8h**).* Compound **8h** was prepared from 4-(4-(chloromethyl)-1-phenyl-1*H*-pyrazol-3-yl)benzonitrile (**6h**) (0.5 g, 1.7 mmol) and was obtained as a white crystalline solid after recrystallization from EtOH/H_2O 1:1 v/v, yield 0.23 g (42%). Mp 162−165 °C. TLC (1:1 petroleum ether/EtOAc), R_f = 0.08. ^{1}H NMR (DMSO-d_6): δ 8.65 (s, 1H, triazole), 8.59 (s, 1H, triazole), 8.01−7.94 (m, 3H), 7.89 (d, J = 7.7 Hz, 2H, Ar), 7.53 (t, J = 8.0 Hz, 2H, Ar), 7.37 (t, J = 7.4 Hz, 1H, Ar), 5.58 (s, 2H, CH_2). ^{13}C NMR ($CDCl_3$): δ 152.1 (CH, triazole), 149.1 (C, pyrazole), 144.5 (CH, triazole), 139.5 (C), 137.3 (C), 133.2 (2 × CH), 130.9 (CH), 130.1 (2 × CH), 128.7 (2 × CH), 127.4 (CH), 119.2 (C), 119.1 (2 × CH), 116.8 (C), 111.2 (C), 43.5 (CH_2). Anal. Calcd for $C_{19}H_{14}N_6$ (326.36): C, 69.93; H, 4.32; N, 25.74. Found: C, 69.80; H, 4.23; N, 25.78.

General Method for the Preparation of 1*H*-Pyrazole-4-carboxamide. Carboxylic acid (**9**) (1 mmol) was dissolved in

DOI: 10.1021/acs.jmedchem.7b01562
J. Med. Chem. 2017, 60, 10257−10267

anhydrous DMF (4 mL/mmol). Then a solution of 1,1′-carbonyldiimidazole (1.1 mmol) in dry DMF (1 mL/mmol) was added, and the reaction was stirred for 1 h. The reaction was cooled to 0 °C; a mixture of 1-(2-ammonioethyl)-1*H*-imidazol-3-ium chloride (**12**) (1 mmol) with triethylamine (3 mmol) in dry DMF (1 mL/mmol) was added, and the mixture stirred at room temperature for 20 h. Once complete, ice-cold H_2O (50 mL/mmol) was added, and the resulting yellow precipitate was collected by filtration, washed with cold water, and dried [15].

*N-(2-(1H-Imidazol-1-yl)ethyl)-1,3-diphenyl-1H-pyrazole-4-carboxamide (**13a**).* Compound **13a** was prepared from 1,3-diphenyl-1*H*-pyrazole-4-carboxylic acid (**9a**) (0.42, 1.6 mmol) and was obtained as a white solid after purification by gradient flash column chromatography, eluted with EtOAc/MeOH 9:1 v/v, yield 0.24 g (40%). Mp 136−138 °C. TLC (9:1 EtOAc/MeOH), R_f = 0.42. ^{1}H NMR (DMSO-d_6): δ 8.90 (s, 1H, pyrazole), 8.37 (s, 1H, NH), 7.88 (d, J = 7.3 Hz, 2H, Ar), 7.79 (d, J = 6.5 Hz, 2H, Ar), 7.65 (s, 1H, imidazole), 7.58 (t, J = 6.8 Hz, 2H, Ar), 7.43 (t, J = 8.2 Hz, 4H, Ar), 7.21 (s, 1H, imidazole), 6.92 (s, 1H, imidazole), 4.16 (s, 2H, CH_2), 3.57 (d, J = 4.6 Hz, 2H, CH_2). ^{13}C NMR (DMSO-d_6): δ 162.9 (CO), 150.9 (C, pyrazole), 138.9, 132.2 (2 × C, Ar), 129.9 (CH, pyrazole), 129.7 (CH, Ar), 129.6 (CH, Ar), 129.1 (CH, Ar), 128.4 (CH, Ar), 128.2 (CH, Ar), 128.2 (CH, Ar), 128.0 (CH, Ar), 127.9 (CH, Ar), 127.7 (CH, pyrazole), 126.9 (CH, Ar), 126.6 (CH, Ar), 118.8 (CH, Ar), 117.4 (C, pyrazole), 45.3, 40.0 (2 × CH_2). Anal. Calcd for $C_{21}H_{19}N_5O$ (357.42): C, 70.57; H, 5.36; N, 19.59. Found: C, 70.28; H, 5.19; N, 19.29.

*N-(2-(1H-Imidazol-1-yl)ethyl)-3-(4-fluorophenyl)-1-phenyl-1H-pyrazole-4-carboxamide (**13b**).* Compound **13b** was prepared from 3-(4-fluorophenyl)-1-phenyl-1*H*-pyrazole-4-carboxylic acid (**9b**) (0.25 g, 1.4 mmol) and was obtained as a white solid after purification by gradient flash column chromatography, eluted with EtOAc/MeOH 9:1 v/v, yield 0.175 g (29%). Mp 158−160 °C. TLC (9:1 CH_2Cl_2/MeOH), R_f = 0.2. ^{1}H NMR (CD_3OD): δ 8.49 (s, 1H, pyrazole), 7.83 (d, J = 7.7 Hz, 2H, Ar), 7.85−7.73 (m, 3H, Ar), 7.56−7.52 (Ψt, J = 7.6, 8.4 Hz, 2H, Ar), 7.41 (t, J = 7.0 Hz, 1H, imidazole), 7.20 (s, 1H, imidazole), 7.19−714 (m, 2H, Ar), 7.05 (s, 1H, imidazole), 4.28 (t, J = 6.0 Hz, 2H, CH_2), 3.72 (t, J = 6.0 Hz, 2H, CH_2). ^{13}C NMR (CD_3OD): δ 166.1 (CO), 165.4 (F−C), 163.5 (C, Ar), 152.4 (C, pyrazole), 140.7 (C, Ar), 131.8, 131.7, 131.1, 129.9, 130.7, 128.9, 128.5 (13 × CH, Ar), 129.8 (C, Ar), 118.1 (C, pyrazole), 47.2, 41.4 (2 × CH_2). Anal. Calcd for $C_{21}H_{18}FN_5O$ 0.3 H_2O (380.81): C, 66.60; H, 4.90; N, 18.31. Found: C, 66.57; H, 4.82; N, 17.99.

*N-(2-(1H-Imidazol-1-yl)ethyl)-3-(4-chlorophenyl)-1-phenyl-1H-pyrazole-4-carboxamide (**13c**).* Compound **13c** was prepared from 3-(4-chlorophenyl)-1-phenyl-1*H*-pyrazole-4-carboxylic acid (**9c**) (0.42 g, 1.4 mmol) and was obtained as a white crystalline solid after recrystallization from acetonitrile, yield 0.11 g (19%). Mp 184−186 °C. TLC (9:1 CH_2Cl_2/MeOH), R_f = 0.13. ^{1}H NMR (CD_3OD): δ 8.53 (s, 1H, pyrazole), 7.83 (d, J = 7.7 Hz, 2H, Ar), 7.72 (d, J = 8.5 Hz, 2H, Ar), 7.68 (s, 1H, imidazole), 7.55 (Ψt, J = 7.6, 8.4 Hz, 2H, Ar), 7.44−7.39 (m, 3H, Ar), 7.18 (s, 1H, imidazole), 7.03 (s, 1H, imidazole), 4.25 (t, J = 6.0 Hz, 2H, CH_2), 3.71 (t, J = 6.0 Hz, 2H, CH_2). ^{13}C NMR (CD_3OD): δ 166.1 (CO), 152.2 (C, pyrazole), 140.7, 135.6, 132.3 (3 × C, Ar), 131.2 (CH, pyrazole), 131.1, 130.8, 129.4, 128.6, 120.5 (12 × CH, Ar), 118.3 (C, pyrazole), 47.1, 41.4 (2 × CH_2). Anal. Calcd for $C_{21}H_{18}ClN_5O$ 0.1 H_2O (393.66): C, 64.07; H, 4.65; N, 17.79. Found: C, 63.92; H, 4.33; N, 17.76.

*N-(2-(1H-Imidazol-1-yl)ethyl)-1-phenyl-3-(p-tolyl)-1H-pyrazole-4-carboxamide (**13d**).* Compound **13d** was prepared from 1-phenyl-3-(*p*-tolyl)-1*H*-pyrazole-4-carboxylic acid (**9d**) (0.47 g, 1.7 mmol) and was obtained as a white solid after purification by gradient flash column chromatography, eluted with EtOAc/MeOH 9:1 v/v, yield 0.034 g (6%). Mp 76−80 °C. TLC (9:1 CH_2Cl_2/MeOH), R_f = 0.20. ^{1}H NMR (CD_3OD): δ 8.50 (s, 1H, pyrazole), 7.81 (d, J = 7.7 Hz, 2H, Ar), 7.69 (s, 1H, imidazole), 7.59 (d, J = 8.1 Hz, 2H, Ar), 7.53 (Ψt, J = 7.7, 8.3 Hz, 2H, Ar), 7.39 (t, J = 7.5 Hz, 1H, Ar), 7.24 (d, J = 8.0 Hz, 2H, Ar), 7.17 (s, 1H, imidazole), 7.03 (s, 1H, imidazole), 4.23 (t, J = 6.0 Hz, 2H, CH_2), 3.68 (t, J = 6.0 Hz, 2H, CH_2), 2.45 (s, 3H, CH_3). ^{13}C NMR (CD_3OD): δ 165.6 (CO), 152.50 (C, pyrazole), 139.98, 139.1 (2 × C, Ar), 130.4 (CH, pyrazole), 129.9, 129.2, 128.3, 119.7 (12 × CH, Ar), 129.8 (C, Ar), 117.4 (C, pyrazole), 46.4, 40.6 (2 × CH_2), 20.6 (CH_3). Anal. Calcd for $C_{22}H_{21}N_5O$ (371.44): C, 71.14; H, 5.70; N, 18.85. Found: C, 70.87; H, 5.74; N, 18.67.

*N-(2-(1H-Imidazol-1-yl)ethyl)-3-(4-methoxyphenyl)-1-phenyl-1H-pyrazole-4-carboxamide (**13e**).* Compound **13e** was prepared from 3-(4-methoxyphenyl)-1-phenyl-1*H*-pyrazole-4-carboxylic acid (**9e**) (0.4 g, 1.4 mmol) and was obtained as a yellow solid after purification by gradient flash column chromatography, eluted with EtOAc/MeOH 9:1 v/v, yield 0.18 g (32%). Mp 108−112 °C. TLC (9:1 CH_2Cl_2/MeOH), R_f = 0.60. ^{1}H NMR (CD_3OD): δ 8.51 (s, 1H, pyrazole), 7.83 (d, J = 7.7 Hz, 2H, Ar), 7.66 (s, 1H, imidazole), 7.55 (Ψt, J = 7.6, 8.4 Hz 2H, Ar), 7.42−7.27 (m, 4H, Ar/imidazole), 7.16 (s, 1H, imidazole), 7.01−6.98 (m, 2H, Ar), 4.25 (t, J = 6.0 Hz, 2H, CH_2), 3.86 (s, 3H, OCH_3), 3.71 (t, J = 6.0 Hz, 2H, CH_2). ^{13}C NMR (CD_3OD): δ 166.3 (CO), 161.1 (C, Ar), 152, 9 (C, pyrazole), 140.8, 134.8 (2 × C, Ar), 131.2 (CH, pyrazole), 130.7, 130.5, 129.2, 128.5, 122.1, 120.9, 115.4, 115.2 (12 × CH, Ar), 118.5 (C, pyrazole), 55.8 (OCH_3), 47.1, 41.5 (2 × CH_2). Anal. Calcd for $C_{22}H_{21}N_5O_2$ 0.2 H_2O (391.04): C, 67.57; H, 5.51; N, 17.91. Found: C, 67.21; H, 5.25; N, 17.56.

CYP121A1 Spectral Binding Assays for Ligand K_D Determination. The CYP121A1 protein was expressed and purified as described previously.[14] Ligand binding assays were performed by spectrophotometric titration using a Cary 60 UV−visible scanning spectrophotometer (Agilent, UK) and a 1 cm path length quartz cuvette, recording spectra between 250 and 800 nm. Titrations were typically done with 3−5 μM CYP121A1 at 28 °C in a 100 mM potassium phosphate (KPi) buffer and 200 mM KCl with a pH of 7.85 and with 0.004% Triton X-100. Ligand stock solutions were prepared in dimethyl sulfoxide (DMSO). Ligands were added in small volumes (typically 0.05−0.2 μL aliquots) from concentrated stock solutions to the protein in a 1 mL final volume. Spectral measurements were taken before the ligand addition and after the addition of each aliquot of ligand until no further spectral change occurred. Difference spectra at each stage in the titration were obtained by the subtraction of the initial ligand-free enzyme spectrum from the subsequent spectra collected after each addition of ligand. From the difference spectra, a pair of wavelengths were identified and defined as the absorbance maximum (A_{peak}) and minimum (A_{trough}). The overall absorbance change (ΔA_{max}) was calculated by subtracting the A_{trough} value from the A_{peak} value for each spectrum collected after a ligand addition. Graphs of ΔA_{max} against [ligand] were plotted for each titration. Titrations were done in triplicate, and the final K_D value presented was determined as the average value across the three sets. The K_D values were determined by fitting the data using either a standard hyberbolic function (eq 1) or the Hill equation (eq 2) using the Origin software (OriginLab, Northampton, MA).

$$A_{obs} = (A_{max} \times L/(K_d + L)) \quad (1)$$

In eq 1 (the standard hyperbolic function, the Michaelis−Menten function adapted for ligand binding), A_{obs} is the observed absorbance change at ligand concentration L, A_{max} is the maximal absorbance change observed at the apparent ligand saturation, and K_D is the dissociation constant for the binding of the ligand (the substrate concentration at which A_{obs} = 0.5 × A_{max}).

$$A_{obs} = (A_{max} \times L^n)/(K^n + L^n) \quad (2)$$

In eq 2 (the sigmoidal Hill equation), A_{obs} is the observed absorbance change at ligand concentration L, A_{max} is the absorbance change at the apparent ligand saturation, K is the apparent dissociation constant, and n is the Hill coefficient, a value describing the apparent extent of cooperativity observed in ligand binding.

Antimycobacterial Activity Assay. *M. tuberculosis* H_{37}Rv was grown in 7H9 liquid medium with 10% Middlebrook OADC Growth Supplement enrichment (BBL/Becton-Dickinson, Sparks, MD, USA). The bacterial growth occurred at 37 °C until the mid log phase was reached ($OD_{600\ nm}$ = 0.4−0.6). After this period, the bacterial suspensions were prepared as described below and REMA assays were performed. The anti-*M. tuberculosis* activity of the compounds

DOI: 10.1021/acs.jmedchem.7b01562
J. Med. Chem. 2017, 60, 10257−10267

was determined by the REMA (Resazurin Microtiter Assay) method.[15] Stock solutions of the tested compounds (10 μg/mL) were prepared in DMSO and diluted in Middlebrook 7H9 broth supplemented with 10% OADC.

The microdilution of the compounds was performed in 96-well plates to obtain final compound concentration ranges 0.39−100 μg/mL. Rifampicin in the concentration range between 0.004 and 1 μg/mL was added as a control. Bacterial suspensions were prepared, and their turbidities were adjusted to match the optical density of the McFarland no. 1 standard. After a further dilution of 1:20 in the Middlebrook 7H9 broth supplemented with OADC, 100 μL of the inoculum was added to each well of the 96-well plate. Cultures were incubated for 7 days at 37 °C, and 30 μL of 0.01% resazurin was added. Wells were read after 24 h for color change, and the fluorescence was measured (excitation/emission of 530/590 nm filters, respectively) in a microfluorimeter. The MIC was defined as the lowest concentration resulting in 90% inhibition of *M. tuberculosis* growth. The presented results are from two independent experiments.

Molecular Modeling and Docking. Docking studies were performed using the MOE[16] program and Mtb CYP121A1 cocrystallized with fluconazole (pdb 2IJ7). All minimizations were performed with MOE until a RMSD gradient of 0.01 kcal/mol/A with MMFF94 force field and partial charges were automatically calculated. The charge of the heme iron at a physiological pH was set to 3^+ (geometry d2sp3) through the atom manager in MOE. The Alpha Triangle placement, which derives poses by random superposition of ligand atom triplets through alpha sphere dummies in the receptor site, was chosen to determine the poses. The London ΔG scoring function estimates the free energy of binding of the ligand from a given pose. Refinement of the results was done using the MMFF94 force field, and rescoring of the refined results using the London ΔG scoring function was applied. The output database dock file was created with different poses for each ligand and arranged according to the final score function (S), which is the score of the last stage that was not set to zero.

Crystallography Studies on CYP121A1. Untagged CYP121A1 protein and crystals were prepared as previously reported, with the following adaptations.[14] Crystals were prepared using a Mosquito pipetting robot (Molecular Dimensions, Newmarket, UK) in 800 nL drops with protein-to-mother liquor at a ratio of 1:1, by vapor diffusion in 1.5−2.1 M ammonium sulfate and 0.1 M sodium MES, or Cacodylate from pH 5.5−6.15. Co-crystals were prepared following incubation with 2 mM ligand prepared in DMSO. Protein solutions were centrifuged at 14,000 rpm for 20 min at 4 °C immediately before crystallogenesis. Ligand soaks were also carried out either by directly dissolving solid ligand to saturation, or by the addition of a 2−5 mM ligand solution in DMSO to the mother liquor, and soaking was carried out for a minimum period of 24 h. Crystals were immersed in mother liquor supplemented with 10−30% oil as cryoprotectant, and cryoprotected and flash-cooled in liquid nitrogen. Data were collected on beamline i02 (wavelength 0.9795 Å) at the Diamond Light Source Facility (Harwell, UK). The diffraction data were reduced, scaled and merged using XDS or Xia2.[18,19] Structures were refined using PHENIX[20] with the native CYP121A1 structure (PDB 1N40)[14] as the starting model. Structural rebuilding and validation were performed with COOT,[21] Molprobity,[22] and PDB REDO.[23]

■ ASSOCIATED CONTENT

Supporting Information

The Supporting Information is available free of charge on the ACS Publications website at DOI: 10.1021/acs.jmedchem.7b01562.

Molecular formula strings (CSV)

Accession Codes

PDB codes for CYP121A with **7b** and **7e** bound are 5OPA and 5OP9, respectively. The authors will release the atomic coordinates and experimental data upon article acceptance for publication.

■ AUTHOR INFORMATION

Corresponding Author

*E-mail: simonsc@cardiff.ac.uk. Phone: +44-(0)-2920-876307.

ORCID

Andrew W. Munro: 0000-0002-4642-180X

Claire Simons: 0000-0002-9487-1100

Notes

The authors declare no competing financial interest.

■ ACKNOWLEDGMENTS

We thank the Cultural Attaché, Libyan Embassy, London and Misurata University for a Ph.D. scholarship to IMT, the Egyptian Government for a research scholarship to HEAEE, and the EPSRC Mass Spectrometry Centre, Swansea, U.K. for mass spectroscopy data. For L.M., we thank his funders FAPESP (2011/21232-1), CNPQ (140079/2013-0), and CAPES PDSE (99999.003125/2014-09). A.W.M., C.W.L., and K.J.M. are grateful to the UK Biotechnology and Biological Sciences Research Council (BBSRC) for the funding through grants BB/I020160/1 and BB/I019227/1. S.S. and L.P.S.C. thank the Francis Crick Institute, which receives its core funding from Cancer Research UK (FC001060), the UK Medical Research Council (FC001060), and the Wellcome Trust (FC001060), and also the Wellcome Trust for a new investigator award to L.P.S.C. (104785/B/14/Z).

■ ABBREVIATIONS USED

Mtb, *Mycobacterium tuberculosis*; Cyy, cyclodipeptide dicyclotyrosine; MDR, multidrug resistant; XDR, extremely drug resistant; TDR, totally drug resistant; REMA, Resazurin Microtiter Assay; MOE, Molecular Operating Environment

■ REFERENCES

(1) World Health Organization. Global Tuberculosis Report 2015. http://www.who.int/mediacentre/factsheets/fs104/en/ (accessed Aug 9, 2017).

(2) Zumla, A.; Nahid, P.; Cole, S. T. Advances in the development of new tuberculosis drugs and treatment regimens. *Nat. Rev. Drug Discovery* **2013**, *12*, 388−404.

(3) McLean, K. J.; Dunford, A. J.; Neeli, R.; Driscoll, M. D.; Munro, A. W. Structure, function and drug targeting in *Mycobacterium tuberculosis* cytochrome P450 systems. *Arch. Biochem. Biophys.* **2007**, *464*, 228−240.

(4) Daniel, T. M. The history of tuberculosis. *Respir. Med.* **2006**, *100*, 1862−1870.

(5) Millard, J.; Ugarte-Gil, C.; Moore, D. A. J. Multidrug resistant tuberculosis. *Br. Med. J.* **2015**, *350*, h882.

(6) McLean, K. J.; Carroll, P.; Lewis, D. G.; Dunford, A. J.; Seward, H. E.; Neeli, R.; Cheesman, M. R.; Marsollier, L.; Douglas, P.; Smith, W. E.; Rosenkrands, I.; Cole, S. T.; Leys, D.; Parish, T.; Munro, A. W. Characterization of active site structure in CYP121. *J. Biol. Chem.* **2008**, *283*, 33406−33416.

(7) Hudson, S. A.; McLean, K. J.; Surade, S.; Yang, Y.; Leys, D.; Ciulli, A.; Munro, A. W.; Abell, C. Application of fragment screening and merging to the discovery of inhibitors of the *Mycobacterium tuberculosis* cytochrome P450 CYP121. *Angew. Chem.* **2012**, *124*, 9445−9450.

(8) Belin, P.; Le Du, M. H.; Fielding, A.; Lequin, O.; Jacquet, M.; Charbonnier, J. B.; Lecoq, A.; Thai, R.; Courçon, M.; Masson, C.; Dugave, C.; Genet, R.; Pernodet, J. L.; Gondry, M. Identification and structural basis of the reaction catalyzed by CYP121, an essential cytochrome P450 in *Mycobacterium tuberculosis*. *Proc. Natl. Acad. Sci. U. S. A.* **2009**, *106*, 7426−7431.

DOI: 10.1021/acs.jmedchem.7b01562
J. Med. Chem. 2017, 60, 10257−10267

(9) Yadlapalli, R. K.; Chourasia, O. P.; Vemuri, K.; Sritharan, M.; Perali, R. S. Synthesis and in vitro anticancer and antitubercular activity of diarylpyrazole ligated dihydropyridines possessing lipophilic carbamoyl group. *Bioorg. Med. Chem. Lett.* **2012**, *22*, 2708−2711.
(10) Desai, N. C.; Joshi, V. V.; Rajpara, K. M.; Vaghani, H. V.; Satodiya, H. M. Facile synthesis of novel fluorine containing pyrazole based thiazole derivatives and evaluation of antimicrobial activity. *J. Fluorine Chem.* **2012**, *142*, 67−78.
(11) Bratenko, M. K.; Chornous, V. A.; Vovk, M. V. 4-Functionally substituted 3-heterylpyrazoles: VIII. 3-Aryl(heteryl)-4-hydroxyl-(chloro)methylpyrazoles. *Russ. J. Org. Chem.* **2002**, *38*, 411−414.
(12) Bratenko, M. K.; Chornous, V. A.; Vovk, M.V. 4-Functionally substituted 3-heterylpyrazoles: III. 3-Aryl (heteryl) pyrazole-4-carboxylic acids and their derivatives. *Russ. J. Org. Chem.* **2001**, *37*, 552−555.
(13) Popkov, S. V.; Skvortsova, M. N. A new method for the synthesis of *n*-(2-aminoethyl)azoles by alkylation of azoles with 2-alkyl-4,5-dihydrooxazoles. *Russ. Chem. Bull.* **2006**, *55*, 1848−51.
(14) McLean, K. J.; Marshall, K. R.; Richmond, A.; Hunter, I. S.; Fowler, K.; Kieser, T.; Gurcha, S. S.; Besra, G. S.; Munro, A. W. Azole antifungals are potent inhibitors of cytochrome P450 mono-oxygenases and bacterial growth in mycobacteria and streptomycetes. *Microbiology* **2002**, *148*, 2937−2949.
(15) Palomino, J. C.; Martin, A.; Camacho, M.; Guerra, H.; Swings, J.; Portaels, F. Resazurin microtiter assay plate: simple and inexpensive method for detection of drug resistance in *Mycobacterium tuberculosis*. *Antimicrob. Agents Chemother.* **2002**, *46*, 2720−2722.
(16) *Molecular Operating Environment (MOE)*, 2013.08; Chemical Computing Group Inc.: 1010 Sherbooke St. West, Suite #910, Montreal, QC, Canada, H3A 2R7, 2016.
(17) Ghose, A. K.; Crippen, G. M. Atomic physicochemical parameters for three-dimensional-structure-directed quantitative structure-activity relationships. 2. Modeling dispersive and hydrophobic interactions. *J. Chem. Inf. Model.* **1987**, *27*, 21−35.
(18) Kabsch, W. XDS. *Acta Crystallogr., Sect. D: Biol. Crystallogr.* **2010**, *66*, 125−132.
(19) Winter, G. Xia2: an expert system for macromolecular crystallography data reduction. *J. Appl. Crystallogr.* **2010**, *43*, 186−190.
(20) Adams, P. D.; Afonine, P. V.; Bunkóczi, G.; Chen, V. B.; Davis, I. W.; Echols, N.; Headd, J. J.; Hung, L.-W.; Kapral, G. J.; Grosse-Kunstleve, R. W.; McCoy, A. J.; Moriarty, N. W.; Oeffner, R.; Read, R. J.; Richardson, D. C.; Richardson, J. S.; Terwilliger, T. C.; Zwart, P. H. Phenix: A comprehensive python-based system for macromolecular structure solution. *Acta Crystallogr., Sect. D: Biol. Crystallogr.* **2010**, *66*, 213−221.
(21) Emsley, P.; Lohkamp, B.; Scott, W. G.; Cowtan, K. Features and development of Coot. *Acta Crystallogr., Sect. D: Biol. Crystallogr.* **2010**, *66*, 486−501.
(22) Chen, V. B.; Arendall, W. B., 3rd; Headd, J. J.; Keedy, D. A.; Immormino, R. M.; Kapral, G. J.; Murray, A. J.; Richardson, J. S.; Richardson, D. C. MolProbity: all-atom structure validation for macromolecular crystallography. *Acta Crystallogr., Sect. D: Biol. Crystallogr.* **2010**, *66*, 12−21.
(23) Joosten, R. P.; Long, F.; Murshudov, G. N.; Perrakis, A. The PDB_REDO server for macromolecular structure model optimization. *IUCrJ* **2014**, *1*, 213−220.

DOI: 10.1021/acs.jmedchem.7b01562
J. Med. Chem. 2017, 60, 10257−10267